JACS
JOURNAL OF THE AMERICAN CHEMICAL SOCIETY
Communication
pubs.acs.org/JACS

Ultrasensitive Electroanalytical Tool for Detecting, Sizing, and Evaluating the Catalytic Activity of Platinum Nanoparticles

Radhika Dasari, Donald A. Robinson, and Keith J. Stevenson*

Department of Chemistry and Biochemistry, University of Texas at Austin, Austin, Texas 78712, United States

Supporting Information

ABSTRACT: Here we describe a very simple, reliable, low-cost electrochemical approach to detect single nanoparticles (NPs) and evaluate NP size distributions and catalytic activity in a fast and reproducible manner. Single NPs are detected through an increase in current caused by electrocatalytic oxidation of N_2H_4 at the surface of the NP when it contacts a Hg-modified Pt ultramicroelectrode (Hg/Pt UME). Once the NP contacts the Hg/Pt UME, Hg poisons the Pt NP, deactivating the N_2H_4 oxidation reaction. Hence, the current response is a "spike" that decays to the background current level rather than a stepwise "staircase" response as previously described for a Au UME. The use of Hg as an electrode material has several quantitative advantages including suppression of the background current by 2 orders of magnitude over a Au UME, increased signal-to-noise ratio for detection of individual collisions, precise integration of current transients to determine charge passed and NP size, reduction of surface-induced NP aggregation and electrode fouling processes, and reproducible and renewable electrodes for routine detection of catalytic NPs. The NP collision frequency was found to scale linearly with the NP concentration (0.016 to 0.024 $pM^{-1}\,s^{-1}$). NP size distributions of 4−24 nm as determined from the current−time transients correlated well with theory and TEM-derived size distributions.

Because of their unique physical and chemical properties, metal nanoparticles (NPs) have attracted tremendous interest in modern chemical research and found applications in a wide variety of fields such as photochemistry,[1a] electrochemistry,[1b] optics,[1c] and catalysis.[1d] To gain a better understanding of their fundamental properties and optimize their activity for various applications, NPs must be characterized precisely in terms of size, shape, and composition. For example, both the size and shape of NPs have been shown to affect their catalytic activity.[2a,b] Hence, several techniques, such as transmission electron microscopy (TEM), scanning electron microscopy (SEM), atomic force microscopy, UV−vis spectroscopy, surface plasmon resonance, mass spectrometry, dynamic light scattering, and X-ray absorption spectroscopy have been developed to determine the NP size and shape distributions. In recent years, interest in using TEM to determine NP size distributions has increased, especially for NPs that are a few nanometers in size, but the cost and limited accessibility of TEM limits its widespread and routine use for correlating structure−property relationships. A high-throughput analytical method that could detect and evaluate the activity of individual NPs in a routine manner would bypass ensemble-type measurements (e.g., UV−vis spectroscopy) and enable the study of single NP catalysts.

Bard[3a−c] and others[3d] recently reported several electrochemical approaches for detecting single NPs by measuring their impact with the conducting surface of an ultramicroelectrode (UME). For example, Bard and coworkers observed a large current amplification due to electrocatalytic processes (oxidation/reduction of the species present in solution) occurring on the surface of an NP when it collided with an inert UME that otherwise could not electrocatalyze the reaction. Compton and coworkers immobilized redox-active *p*-nitrophenol ligands on metal NPs and monitored the current transients corresponding to reduction of the attached ligands whenever the NPs contacted an electrode that was held at a potential negative enough to reduce *p*-nitrophenol. These methods attempted to quantify current transients to determine NP size distributions, but there are certain aspects associated with the current−time (i−t) response that are not fully understood. Two types of i−t responses have been observed: a current step[3a] that increases with time as a result of NP accumulation and a current "spike" or "blip" that decays to the background current level with time.[3b] The NP type and the indicator redox reaction also influence the shape and magnitude of the i−t response for individual NP collisions. For instance, at a Au UME with citrate-capped Pt NPs for N_2H_4 oxidation, a stepwise i−t increase ("staircase" response) was observed, but for IrO_x NPs analyzed for water oxidation, the i−t response appeared as a "spike." The staircase i−t response suggests that the NP sticks to the electrode upon contact, and further collisions contribute to a buildup of electrocatalytic NPs and an overall increase in current. In this case, the signal-to-noise (S/N) ratio changes with time and each new collision event, thereby making it difficult to detect individual NP collisions over long analysis times and to determine whether other processes are involved, such as surface-induced NP aggregation or electrode fouling (Figure S1 in the Supporting Information). The spike-shaped i−t response observed in the case of water oxidation with IrO_x NPs at a Au UME suggests that the collisions are elastic (i.e., the NP bounces off rather than sticking on the surface). However, the current spike could also be associated with NP deactivation processes (e.g., poisoning). Until now, this kind of current response has been limited to IrO_x NPs at a Au UME for water oxidation and to *p*-nitrophenol-labeled NPs, where there is

Received: October 28, 2012
Published: December 27, 2012

dx.doi.org/10.1021/ja310614x | *J. Am. Chem. Soc.* 2013, 135, 570−573

always an issue of electroactive surface coverage of the redox-active molecule on the NP. Here we report an electrochemical approach utilizing a renewable Hg-modified Pt (Hg/Pt) UME as a reliable and robust electrode platform for detecting and screening NP sizes that overcomes all of the issues associated with the above-described electrochemical methods, such as electrode fouling and accumulative NP sticking processes. While Hg drop electrodes have been used previously to study adhesion processes for liposomes, montmorillonite particles, and TiO_2 particles,[4a−d] this is the first report describing the use of a Hg thin-film UME to detect single NP collisions associated with Faradaic electrocatalytic processes.

Our approach has several distinct advantages for quantitative analysis of single NP electrocatalysts. The key advance is the use of a Hg/Pt UME as the working electrode. We benchmarked this method using citrate-capped Pt NPs of different sizes synthesized by a well-established recipe[5] with N_2H_4 oxidation as the electrocatalytic indicator reaction. Figure 1 shows a schematic

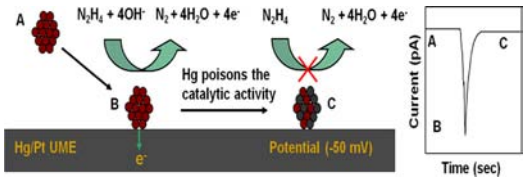

Figure 1. Schematic representation of a single Pt NP collision event at a Hg/Pt UME and the current enhancement by electrocatalytic oxidation of N_2H_4.

representation of the detection of single Pt NPs via electrocatalytic amplification using N_2H_4 oxidation at a Hg/Pt UME as the indicator. The Hg/Pt UME is held at a potential where it does not catalyze the reaction (region A). When a NP diffuses to the UME and either collides with it or is at a distance where electrons can tunnel to it, the electrocatalytic reaction is turned on, resulting in an increase in current (region B). Once the Pt NP contacts the Hg/Pt UME, it appears that Hg poisons the Pt NP and turns off the catalytic reaction, resulting in a decrease in current, which eventually drops back to the background level (region C). As a result, a distinct current spike with a high S/N ratio is observed for single NP collisions at the Hg/Pt UME. This response is unlike the staircase current response previously observed at a Au UME.[3a] While the use of Hg^0 as a catalyst poison to suppress the catalytic activity of bulk Pt has been known for several decades,[6] its use to improve the detection of single NPs has not been reported to date. We attribute the poisoning process to either physisorption of Hg on Pt or Hg−Pt amalgamation. Though bulk amalgamation of Pt with Hg has been generally disregarded, there are a few reports of Hg−Pt amalgamation and Hg−Pt alloy formation at electrodes, resulting in a different electrochemical response than for pure Pt or Hg electrodes.[7a,b]

Figure 2A shows the i−t plot recorded at a Hg/Pt UME held at a potential of −0.05 V in a 50 mM phosphate buffer (pH ∼7.5) containing 15 mM N_2H_4 before the injection of Pt NPs. The background current was ∼150 pA and remained constant over the time course of the experiment, unlike the background current at a Au UME, which decays quickly with time.[3a] Also, the background current at the Hg/Pt UME was 2 orders of magnitude lower than the current observed on a Au UME of similar diameter (∼2×10^{-8} A). In an i−t curve recorded at the same Hg/Pt UME after injection of Pt NPs, very distinct current

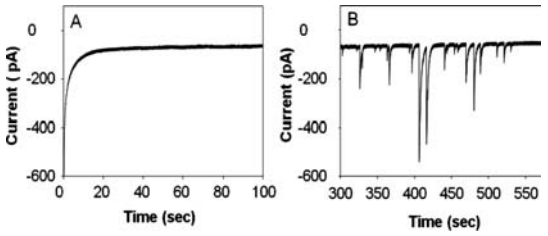

Figure 2. Chronoamperometric plots recorded at a Hg/Pt UME (radius 12.5 μm) in 50 mM phosphate buffer (pH ∼7.5) containing 15 mM N_2H_4 (A) before and (B) after injection of Pt NPs [applied potential (V_{app}), −50 mV vs Ag/AgCl; data acquisition interval (t_{data}), ∼1.5 ms; NP size, ∼25.7 nm; NP concentration, ∼3 pM].

spikes were observed (Figure 2B). Normally, the current spike in a single collision showed a very fast increase and a slower decay, unlike the accumulative increase in current observed at a Au UME. Most of the current spikes were quite uniform in magnitude, although there were some subtle differences in the height and shape of some transients that we attribute to polydispersity in the sizes and shapes of the particular NP sample and small variations in the catalytic response and poisoning processes. In a control experiment, we did not observe any distinct current spikes upon introduction of Pt NPs in pH ∼7.5 phosphate buffer solution containing no N_2H_4 (Figure S2), indicating that the NP current transients observed after injection of Pt NPs into buffer containing N_2H_4 were indeed due to N_2H_4 oxidation. Collision experiments were performed under different experimental conditions to confirm that the observed current transients were due to individual Pt NP collisions. For the same colloidal Pt NP solution, the peak current increased with increasing N_2H_4 concentration (Figure S3). Also, the number of current spikes increased with increasing NP concentration (Figure 3A), as would be expected if the observed current

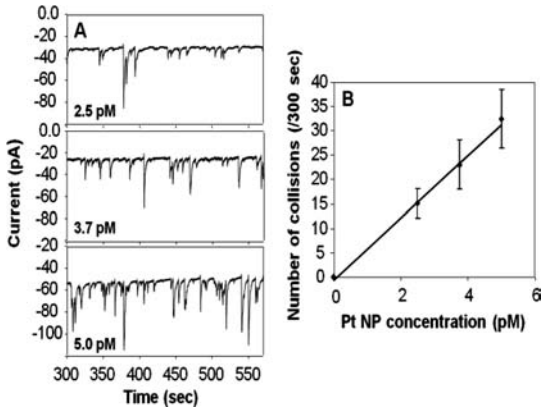

Figure 3. (A) Chronoamperometric plots for single Pt NP collisions at a Hg/Pt UME (radius 12.5 μm) in 50 mM phosphate buffer (pH ∼7.5) containing 15 mM N_2H_4 and various concentrations of Pt NPs (V_{app}, −50 mV vs Ag/AgCl; t_{data}, ∼1.5 ms; Pt NP size ∼4.7 nm), and (B) Correlation between the number of collisions and the Pt NP concentration from three replicate measurements.

transients are due to individual NP collisions. The collision frequency scaled linearly with concentration (Figure 3B) and is found to be 0.016 to 0.024 pM^{-1} s^{-1} which is in good agreement with the value 0.012−0.02 pM^{-1} s^{-1} reported before by Bard and coworkers.[3a] The lowest concentration of Pt NPs that we could detect within a 300 s time interval using our approach was 0.7 pM. The observed collision frequency corresponds to an NP

dx.doi.org/10.1021/ja310614x | J. Am. Chem. Soc. 2013, 135, 570−573

diffusion coefficient of $\sim 2 \times 10^{-8}$ cm^2/s, which is lower than the diffusion coefficient estimated using the Stokes−Einstein relation ($\sim 1 \times 10^{-7}$ cm^2/s), perhaps because some of the NPs that collide with electrode actually do not stick to it and generate a current response. We also tested the reproducibility and reusability of the Hg/Pt UME. Figure S4 shows *i*−*t* plots for single Pt NP collisions at the Hg/Pt UME recorded for 1000 s. We were able to see current spikes over the entire 1000 s window, indicating that the electrode does not foul. Figure S5A shows three *i*−*t* plots for single Pt NP collisions recorded sequentially at the same Hg/Pt UME. The background current and the frequency of collisions did not change significantly even after multiple collisions were observed, indicating that the Hg/Pt electrode can be reused and does not foul over long analysis times. Figure S5A,B shows *i*−*t* plots for single Pt NP collisions recorded at two different Hg/Pt UMEs. We observed similar background currents, collision frequencies, and charges passed per spike, indicating that our method is reproducible. To confirm our hypothesis that Pt NPs form an amalgam with Hg upon contact with the Hg/Pt UME, turning off the electrocatalytic N_2H_4 oxidation, we tried to load the Hg/Pt UME with Pt NPs and image them over time using SEM to track morphology changes that would indicate amalgam formation. Figure S6 shows SEM images of the Pt/Hg UME loaded with Pt NPs obtained on the same day and after 16 days. We did not see any significant changes in the structure of the electrode or the Pt NPs, which could mean that the amalgamation process was instantaneous and occurred before the SEM image was acquired or possibly that the morphology change due to amalgamation was so small that it could not be observed with SEM.

Hence, we performed several other experiments, such as N_2H_4 oxidation at a Hg/Pt UME before and after loading with Pt NPs and collision experiments with prepoisoned Pt NPs, to prove the possibility of Pt NP deactivation due to amalgamation. We did not see any difference in N_2H_4 oxidation at the Hg/Pt UME before and after loading with Pt NPs (Figure S1B), which indicates that Pt NPs are deactivated after they stick to the Hg/Pt UME. Also, no current transients due to single NP collisions were observed when bulk Hg was added to the Pt NP solution before performing collision experiments, meaning that Pt NPs were prepoisoned (Figure S7). These observations do not completely rule out the possibility that Pt NPs bounce back into the solution, but they do support our hypothesis that the Pt NPs are deactivated after they stick to the Hg/Pt UME. An in-depth investigation of the mechanism involved in observing single NP collisions at the Hg/Pt UME is one of our prime interests in future studies.

We also tested the applicability of our approach as an analytical tool for screening NP sizes. If the observed current transients are due to individual NP collisions, we should be able to determine the Pt NP size distribution from the distribution of peak currents at constant N_2H_4 concentration. Three colloidal solutions containing Pt NPs of different sizes were tested. Figure 4A−C shows TEM images of the Pt colloidal solutions, and the histograms in Figure 5A−C show the NP size distributions determined from the TEM images. The average sizes of the NPs were determined to be 4.7 ± 1.0, 14.1 ± 2.3, and 25.7 ± 2.6 nm, respectively. Figure 4D−F shows representative *i*−*t* profiles recorded for the corresponding colloidal solutions. Other than the NP size, all of the other parameters were kept constant, so any differences in the current events were due to differences in NP size and size polydispersity. The *i*−*t* plots recorded for the three solutions showed discrete current spikes with different current

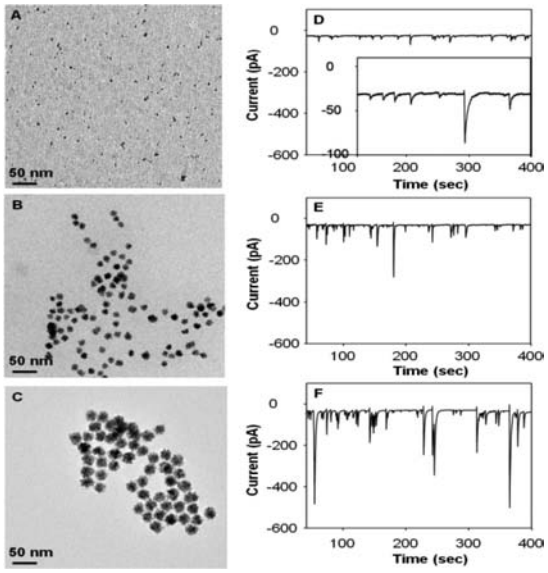

Figure 4. (A−C) TEM images of Pt NP colloidal solutions containing various sizes of Pt NPs and (D−F) corresponding chronoamperometric plots for single Pt NP collisions at a Hg/Pt UME (radius 12.5 μm) in 50 mM phosphate buffer (pH ~7.5) containing 15 mM N_2H_4 and ~3 pM NPs (V_{app}, −50 mV vs Ag/AgCl; t_{data}, ~1.5 ms).

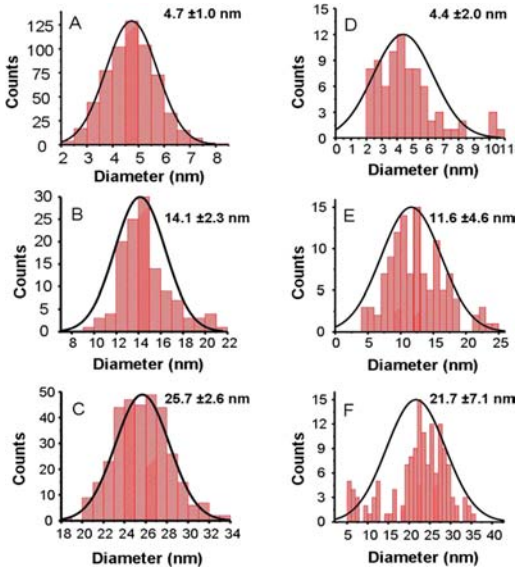

Figure 5. Histograms showing statistical size distributions of NPs for three different Pt colloidal solutions containing different NP sizes, as determined from (A−C) TEM and (D−F) *i*−*t* plots by integration of the charge passed per spike during single NP collisions.

amplitudes. The total charges passed per spike during a single NP collision event was concentrated over the range of 40−70, 80−185, and 155−329 pC, respectively for the three Pt colloidal solutions containing various sizes of NPs (Figure S8). The average charge per spike during a single NP collision scaled linearly with the average NP diameter as determined from TEM (Figure 6). Using the reported equation for calculating the amplitude of the mass-transfer-limiting current generated at an individual spherical metal NP in contact with a planar electrode,[3a] we estimated the corresponding sizes of the NPs from the *i*−*t* plots. These calculations were based on the assumptions that the integrated charge passed per spike

dx.doi.org/10.1021/ja310614x | J. Am. Chem. Soc. 2013, 135, 570−573

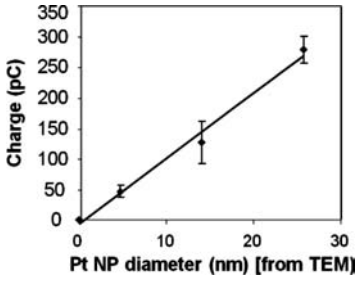

Figure 6. Average charge passed per spike during single NP collisions vs average NP size determined from TEM.

corresponds to the current amplitude and the potential is held at the mass-transfer-limiting regime. Hence, the particle sizes determined from the current transients might be slightly biased and are underestimations. The histograms in Figure 5D−F show the size distributions of NPs obtained from the *i*−*t* plots shown in Figure 4D−F. The average Pt NP sizes were 4.4 ± 2.0, 11.6 ± 4.6, and 21.7 ± 7.0 nm, respectively, which are smaller and possess larger deviations than the TEM results but are within the range determined by TEM. We note that even though the equation used to estimate the Pt NP size based on the integrated charge fails to take into account the time-dependent decay of the current, we still observed a good correlation between the sizes determined from the *i*−*t* plots and TEM. This could reflect the fact that when the Pt NP just makes contact with the Hg/Pt UME, the total surface area of the Pt NP is catalytically active and the resulting initial peak-to-peak amplitude is probably equal to the diffusion-limited current. Though the NP gets deactivated by possible amalgamation and the current eventually drops to the background level, this process probably is so sluggish that the initial peak-to-peak amplitude greatly influences the charge integral, which likely explains the good correlation between the sizes determined from the *i*−*t* plots and TEM. In our case, the initial peak-to-peak amplitude could be slightly lower than the diffusion-limited current, as we assumed the system to be in the mass-transfer-limited region, but we still think it greatly influences the charge integral. Also, instrumental limits such as the sampling interval can affect the current amplitude. If the deactivation process is faster than the sampling interval, a lower current would be obtained, which would in turn affect the Pt NP radius estimated from the integrated charge. Though we used the fastest possible sampling interval (1.5 ms) in our experiments, the limited time response could still affect the measured current, possibly explaining why the charge-derived sizes are slightly smaller than those determined by TEM. We also determined the root-mean-square (rms) noise and S/N ratio from the analysis of current transients. The rms noise was found to be in the range 0.41−0.71 pA with a steady low noise level maintained over long analysis times (>1000 s). As a result, the S/N ratio increased with increasing NP size, from ∼18 to 351 and 1116 for 4.7, 14.1, and 25.7 nm Pt NPs, respectively. From this analysis, we estimate that the size of the smallest Pt NPs that can be detected using our approach is ∼1.6 nm.

In conclusion, we have successfully demonstrated the use of a Hg/Pt UME as an electrode platform for detecting and screening NP sizes. By employing Hg/Pt as an electrode, we were able to observe a consistent spike-shaped current response for single NPs collisions with a low background current, leading to a better S/N ratio and more precise quantitative analysis. Analysis of very small current transients suggested that we should routinely be able to detect particles smaller than 2 nm. Since we observed a very good correlation between the sizes determined by our approach and TEM, we think that our approach is definitely quicker and simpler than TEM for detecting and determining size distributions of Pt NPs. Besides being a quantitative tool for determining NP size and size distributions, our approach has potential use in electroanalysis for detecting various analytes and studying the kinetics of isolated single NP electrocatalysts. These studies will be reported in due course.

■ ASSOCIATED CONTENT

Ⓢ Supporting Information

Experimental details and additional data. This material is available free of charge via the Internet at http://pubs.acs.org.

■ AUTHOR INFORMATION

Corresponding Author

stevenson@cm.utexas.edu

Notes

The authors declare no competing financial interest.

■ ACKNOWLEDGMENTS

We thank the DTRA (Grant HDTRA1-11-1-0005) for support and Dr. Richard M. Crooks for valuable discussions. R.D. acknowledges Nellymar Membreno for acquiring TEM images.

■ REFERENCES

(1) (a) Rao, C. N. R.; Kulkarni, G. U.; Thomas, P. J.; Edwards, P. P. *Chem. Soc. Rev.* **2000**, *29*, 27. (b) Henglein, A. *Chem. Rev.* **1989**, *89*, 1861. (c) Schmid, G.; Chi, L. F. *Adv. Mater.* **1998**, *10*, 515. (d) Lewis, L. N. *Chem. Rev.* **1993**, *93*, 2693.

(2) (a) Shao, M.; Peles, A.; Shoemaker, K. *Nano Lett.* **2011**, *11*, 3714. (b) Sánchez-Sánchez, C. M.; Solla-Gullon, J.; Vidal-Iglesias, F. J.; Aldaz, A.; Montiel, V.; Herrero, E. *J. Am. Chem. Soc.* **2010**, *132*, 5622.

(3) (a) Xiao, X.; Fan, F.-R. F.; Zhou, J.; Bard, A. J. *J. Am. Chem. Soc.* **2008**, *130*, 16669. (b) Kwon, S. J.; Fan, F.-R. F.; Bard, A. J. *J. Am. Chem. Soc.* **2010**, *132*, 13165. (c) Zhou, H.; Park, J. H.; Fan, F.-R. F.; Bard, A. J. *J. Am. Chem. Soc.* **2012**, *134*, 13212. (d) Zhou, Y.-G.; Rees, N. V.; Compton, R. G. *Chem. Commun.* **2012**, *48*, 2510.

(4) (a) Hellberg, D.; Scholz, F.; Schauer, F.; Weitschies, W. *Electrochem. Commun.* **2002**, *4*, 305. (b) Hellberg, D.; Scholz, F.; Schubert, F.; Lovrić, M.; Omanović, D.; Hernández, V. A.; Thede, R. *J. Phys. Chem. B* **2005**, *109*, 14715. (c) Schloz, F.; Hellberg, D.; Harnisch, F.; Hummel, A.; Hasse, U. *Electrochem. Commun.* **2004**, *6*, 929. (d) Heyrovsky, M.; Jirkovsky, J.; Struplova-Bartackova, M. *Langmuir* **1995**, *11*, 4300.

(5) Bigall, N. C.; Härtling, T.; Klose, M.; Simon, P.; Eng, L. M.; Eychmüller, A. *Nano Lett.* **2008**, *8*, 4588.

(6) Whitesides, G. M.; Hackett, M.; Brainard, R. L.; Lavalleye, J. P. P. M.; Sowinski, A. F.; Izumi, A. N.; Moore, S. S.; Brown, D. W.; Staudt, E. M. *Organometallics* **1985**, *4*, 1819.

(7) (a) Fertonani, F. L.; Benedetti, A. V.; Ionashiro, M. *Thermochim. Acta* **1995**, *265*, 151. (b) Kemula, W.; Kublik, Z.; Galus, Z. *Nature* **1959**, *184*, 1795.